Kinematic Assessment of Subject Personification of Human Body Models (THUMS).

Ana Piqueras-Lorente, Johan Iraeus, Ana I. Lorente, Francisco J. López-Valdés, Óscar Juste-Lorente, Mario Maza-Frechín, Bengt Pipkorn

Abstract The goal of this study was to quantify the effect of improving the geometry of a human body model on the accuracy of the predicted kinematics for 4 post-mortem human subject sled tests. Three modifications to the computational human body model THUMS were carried out to evaluate if subject personification can increase the agreement between predicted and measured kinematics of post-mortem human subjects in full frontal and nearside oblique impacts**.** The modifications consisted of: adjusting the human body model mass to the actual subject mass, morphing it to the actual anthropometry of each subject and finally adjustment of the model initial position to the measured position in selected post-mortem human subject tests.

A quantitative assessment of the agreement between predicted and measured response was carried out by means of CORA analysis by comparing the displacement of selected anatomical landmarks (head CoG, T1 and T8 vertebre and H-Point).

For all three scenarios, the more similar the human body model was to the anthropometry and posture of the sled tested post-mortem human subject, the more similar the predictions were to the measured responses of the post-mortem human subject, resulting in higher CORA score.

Keywords biomechanics, biofidelity, simulation, subject personification, THUMS

I. INTRODUCTION

Several Finite Element Human Body Models (FE-HBM) have been developed to predict the response of the human body under blunt impacts. However, the commercially available models such as THUMS, from Toyota Motor Corporation and Toyota Central R&D [1] and GHBMC from the Global Human Body Model Consortium [2] represent a limited number of anthropometric sizes (95th percentile male, 50th percentile male and 5th percentile female are the most common sizes) and they are only available in a standard seated position for the vehicle occupant or standing posture for the pedestrian [3]. Due to the anthropometric and pre-impact posture variability of real humans, to mimic the impact response of specific subjects, it is suggested that human body models should be *personalised*. The personification of human body models can for example be done by modifying the mass or the geometry (both external and internal). For HBMs based on the FE method, this could be carried out by modifying material properties or nodal coordinates through morphing. Previous work has been done by [4]-[7] with such modifications in frontal and side impacts.

The morphing was carried out by means of Kriging interpolation. The module was included in the PIPER v1.0.0 software [8]PIPER EU project, “piper-project.org” [http://www.piper-project.org/], 2017/11/10 [2018/01/11].. The PIPER software can estimate the missing dimensions based on a selected database (ANSUR; SNYDER or CCTANTHRO) using certain known anthropometry values as input variables. The ANSUR database includes adult anthropometry values measured in supine and seated position.

The aim of this study is to evaluate if model modifications using subject personification techniques increases the similarity between the predicted kinematic responses of a human body model (HBM) and the measured response from post-mortem human subjects (PMHSs) in frontal and nearside oblique impacts using contemporary restraints. The agreement between the predicted and the measured response was quantified using CORA (correlation and analysis) rating [9].

Ana Piqueras (+34 635 38 94 61, apiquera@unizar.es) , Ana I. Lorente and Óscar Juste-Lorente are PhD students and Mario Maza-Frechín is Associative Professor at the Impact Laboratory (I3A) at University of Zaragoza, Spain. Johan Iraeus is PhD at the Mechanics and Maritime Sciences department at Chalmers University of Technology in Gothenburg, Sweden. Francisco J. López-Valdés is Assistant Professor and Research Associate, Instituto de Investigación Tecnológica (IIT), ICAI, Universidad Pontificia de Comillas. Madrid, Spain. Bengt Pipkorn is Director of Simulation and Active structures at Autoliv Research, Vårgårda, Sweden and Adjunct Professor at Chalmers University of Technology in Gothenburg, Sweden.

II. METHODS

A modified version of THUMS v3 model [10] was used in this study. Modifications included remodelling of the ribcage [11] and recalibration of the lumbar spine properties [12]. To evaluate the kinematic response of this HBM, four PMHS sled tests in frontal and frontal oblique load cases were carried out [13]-[14].

The sled test fixture (Gold Standard) consisted of a rigid metallic frame allowing complete visual access to the occupant while preserving the basic geometry of a standard seat of a passenger car. This test fixture was developed as a reasonable approximation to the passenger posture in the development of thoracic injury criteria [15]-[16]. In these tests, the knee bar that was used in the references provided was removed from the fixture. The seat for scenarios 1 and 2 was composed of inclined steel plates designed to restrain the pelvis motion to mimic pelvis kinematics observed in tests with real vehicle seats. In the Scenario 3 the seat consisted on a single horizontal steel plate.

PMHS information and sled test fixtures for the three studied scenarios is shown in Table I.

TABLE I
PMHS INFORMATION AND TEST SET-UP

	SCENARIO 1		SCENARIO 2	SCENARIO 3
PMHS	A	B	C	D
Test	1	2	3	4
Nominal velocity (km/h)	34.1	34.3	34.3	35
Restraint system	3-point seatbelt. Shoulder PT (2kN). Lap PT (3.5kN) and FL (4.5kN)	3-point seatbelt. Shoulder PT (2kN). Lap PT (3.5kN) and FL (4.5kN)	3-point seatbelt. Lap PT (3.5kN) and FL (4.5kN)	2B seatbelt. Shoulder PT (2kN), lap PT (3.5kN) and FL (6kN)
Seat	Inclined steel plates	Inclined steel plates	Inclined steel plates	Horizontal steel plate
Impact angle (º)	30	30	30	0
Age	66	68	60	39
Gender	Male	Male	Male	Male
Stature (cm)	175	169	170.5	181
Seated height (cm)	96.3	103.8	101.4	97
Weight (kg)	47	53	57	62
Cause of death	Pancreatic cancer	Lung cancer	Lung cancer	Cardiac arrest

Instrumentation

The kinematic responses of the subjects from Scenarios 1 and 2 (Table I) were collected at 1 kHz using a 3D motion capture system (Vicon, TS series, Oxford, UK). Retroreflective markers were attached to selected locations of the subject, sled fixture and restraint system. In order to accurately acquire the response of the selected bones and its initial positions, the markers were attached directly to the skull and vertebrae by means of plates screwed directly to the bones. With the geometry of each screwed plate and the corresponding bone morphology (obtained from a computed tomography (CT) scan) the movement of each bone was reconstructed [17] after defining their own Local Coordinates System [18].

For the full-frontal impact configuration, corresponding to the Scenario 3, the kinematic behaviour of the left head external auditory meatus (EAM), left acromion and left tibial condyle in the sagittal plane were tracked from the high speed video recorded at 1,000 fps.

In all three scenarios, four force transducers were installed in the upper and lower shoulder belt and the inner and outer lap belt band, recording the belt forces.

Boundary Conditions

All simulations were carried out in the same conditions for each scenario. Sled acceleration pulses, obtained from the physical tests, were applied to the sled fixture in order to obtain the same loading scenarios. The parameters of the restraint system were adjusted to accurately represent the interaction between the seatbelt and the occupant, taking the belt forces from the real tests as reference.

HBM Personification

The HBM was personalised in three steps. In each step, the level of complexity was increased. First, the overall mass of the HBM was adjusted to the one of the Post Mortem Human Subject (PMHS) of the relevant sled test. Second, the THUMS model was morphed to reflect the individual anthropometry of each PMHS. Third, the postures of the original, mass-scaled and morphed THUMS models were adjusted to the actual positions of the PMHS. These modifications resulted in a total of six versions of the THUMS model for each crash scenario, the baseline model and five modified models with different levels of personification:

1. *Baseline:* The first level was to use the unmodified HBM as it is. The THUMS v3 model represents an occupant with a stature of about 177cm and a body mass of about 77kg.
2. *Scaled mass*: In the second model, the overall mass was adjusted to represent the individual PMHS (Table I) by scaling the density of the outer flesh properties.
3. *Morphed*: The HBM model was morphed to reflect the individual anthropometry and body mass of each PMHS measured before each test. The THUMS model was prepared to be processed by means of a metadata file in which all FE parts were identified and classified as bone, flesh (including muscles, fat, ligaments, etc.), organs and skin parts and divided into six main areas: head, trunk, upper limbs and lower limbs (as shown in Fig. 1). In order to perform the morphing, lengths and contours had to be identified. Lengths was defined as the distance between two landmarks. For this purpose, two nodes of the model had to be identified in the metadata and used as landmarks. The PIPER software created auxiliary control points semi-automatically to define the body contours. The anthropometric dimensions (lengths and contours) in seated position used as input values for each subject were extracted from the seated anthropometry measurements (Table VIII(A), Appendix) and from the captures of the VICON markers before the tests. However, more data was required in order to morph the model accurately especially in Scenario 3, where the seated anthropometry was not available. Values shown on Table VII(A) and Table VIII(A) were entered as input variables and, after the regression analysis, the PIPER software calculated the missing target dimensions.

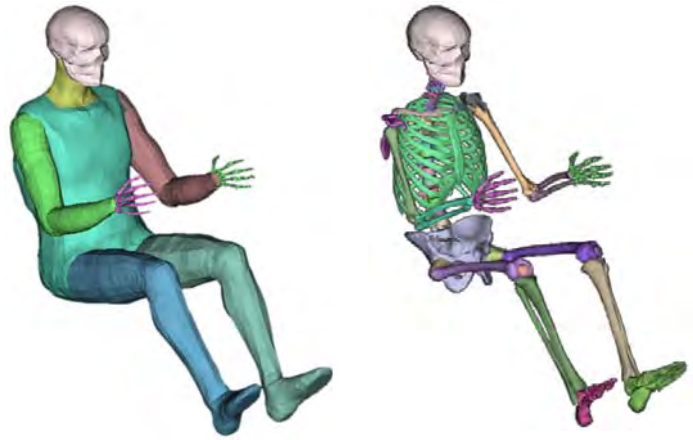

Fig. 1: Visualization of the entities used for the morphing process

4. *Baseline postured*: To analyse the influence of initial posture, the baseline model was modified by aligning the spine curvature of the model to the actual spine curvature of the PMHSs at t=0ms. This was done using a pre-simulation where the displacements of the head CoG, T1, T8 and H-Point were prescribed, to finally conform to the positions measured in the PMHSs.
5. *Scaled mass postured*: In this version of the model, both mass and posture were modified to resemble the weight and posture of the occupant.
6. *Morphed postured*: The posture of the morphed version (3) was adapted with the procedure followed for the model versions 4 and 5.

TABLE II
ANGLE FORMED WITH THE VERTICAL OF
THE SELECTED LANDMARKS IN THE SPINE WITH RESPECT TO THE PREVIOUS

SUBJECT	THUMS	PMHS A	PMHS B	PMHS C		PMHS D
Test	---	1	2	3		4
$\alpha_{Head\text{-}T1}$	-20	-16	-12	-9	$\alpha_{Head\text{-}T1}$	-14
$\alpha_{T1\text{-}T8}$	-25	-30	-25	-28	$\alpha_{T1\text{-}H\text{-}Point}$	26
$\alpha_{T8\text{-}L2}$	38	44	39	40		
$\alpha_{L2\text{-}H\text{-}Point}$	51	60	38	41		

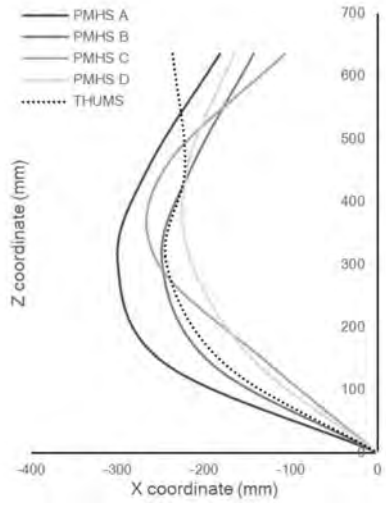

Fig. 2**:** Pre-impact spline alignment of the PMHSs compared with the spine alignment of the baseline THUMS model. The origin of the graph represents the H-Point and the endpoint of each curve represents the head of the subjects.

Quantitative Assessment of the Kinematic Response

The assessment of the different versions of the HBM was done by comparing the trajectories in X, Y and Z-axis of selected anatomical landmarks: head CoG, T1 and T8 vertebrae and H-Point for Scenarios 1 and 2 and left EAM, left shoulder and left knee for Scenario 3. The agreement between the predicted response and the sled test results was quantified using CORA v 4.0.4 [9]. CORA rating is a method to evaluate the time-history signals, the reference curve (physical test) and the predicted response (simulation). CORA uses two methods to calculate the signals correlation taking the physical tests as the reference: The corridor method calculates the deviation of the signal between two curves automatically crated by the CORA software and the cross-correlation method evaluates some specific characteristics of the signal such as phase shift, size and shape. The total CORA score is calculated by adding the weighted ratings obtained from both methods and expressed in a scale from 0 to 1, where 1 represents a perfect correlation and 0 represents no correlation. According to the rating stipulated in ISO/TR 18571 the resultants of the CORA score are classified into four categories: Values above 0.94 are considered excellent, values between 0.94 and 0.8 are good, values between 08 and 0.58 are considered as a fair correlation and values below 0.58 are treated as a poor correlation.

The standard CORA implementation uses equal weighting for all the signals analysed for a load case. However, as the displacement of the analysed body landmarks differs substantially in magnitude (see Table IV(A), Table V(A) and Table VI(A)), i.e., the head displacement during the test was between five and ten times larger than the H-Point displacement, it was considered reasonable to weight the signals accordingly. Therefore, in this study it was chosen to weight the landmarks signals based on the magnitude of the landmark displacement (available in Table IV(A), Table V(A)and Table VI(A))in the CORA analysis. The CORA scores for the individual landmarks and the total

score using the modified weighting factors can be seen in Table I(A), Table II(A) and Table III(A). The weighting factors can be seen in TABLE III.

TABLE III
WEIGHTING FACTORS FOR THE SELECTED LANDMARKS OF EACH CRASH SCENARIO

	SCENARIO 1	SCENARIO 2	SCENARIO 3	
Head	0.483	0.409	Head	0.483
T1	0.261	0.272	Shoulder	0.459
T8	0.203	0.235	Knee	0.058
H-Point	0.053	0.084	Total	1
Total	1	1		

III. **RESULTS**

Displacement plots in transverse and sagittal plane for all simulations are shown in Fig. 1(A), Fig. 2(A) and Fig. 3(A) (see Appendix) and compared with the corresponding physical tests for each crash scenario.
The results of the CORA analysis for all the model versions are shown in Table IV. Quantitatively, the morphed postured version has the highest CORA score in all three scenarios and each personification strategy leads to an improvement in the overall kinematic response compared to the sled tests. The CORA score for the X-axis, Y-axis and Z-axis landmarks displacement is provided in Table I(A), Table II(A) and Table III(A) (see Appendix).

TABLE IV
CORA SCORES FOR THE THREE CRASH SCENARIOS

MODEL VERSION	BASELINE	SCALED MASS	MORPHED	BASELINE POSTURED	SCALED MASS POSTURED	MORPHED POSTURED
Scenario 1	0.644	0.648	0.650	0.664	0.675	0.684
Scenario 2	0.638	0.653	0.688	0.673	0.704	0.715
Scenario 3	0.565	0.637	0.684	0.654	0.679	0.713

Seatbelt forces

The elements selected for the force measurement during the simulation were selected in accordance with the location of the force transducers during the physical tests.
The belt forces recorded during the tests were used to adjust the parameters of the restrain system on the simulations. Peak values due to the pretensioner and the force limiter were established and the load curves were modified to resemble the physical tests for each scenario. The upper shoulder belt forces from the tests and simulations can be observed in Fig. 3.
During the rebound phase, the duration of the force limit value differs depending on the model version. For all three scenarios a longer duration was observed for the baseline and baseline postured versions than the versions in which the mass of the occupant was adjusted, not only during the rebound phase, but also during the loading phase in those cases in which a pretensioner was installed (scenarios 1 and 3).

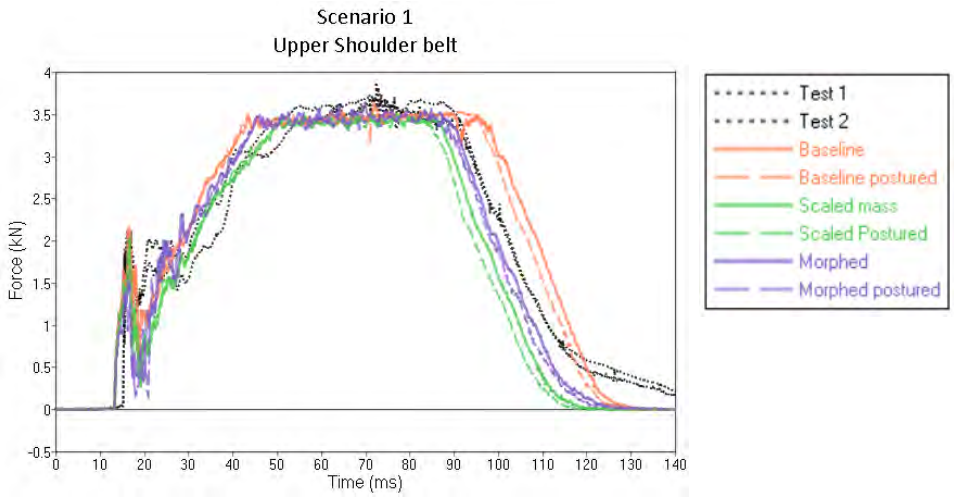

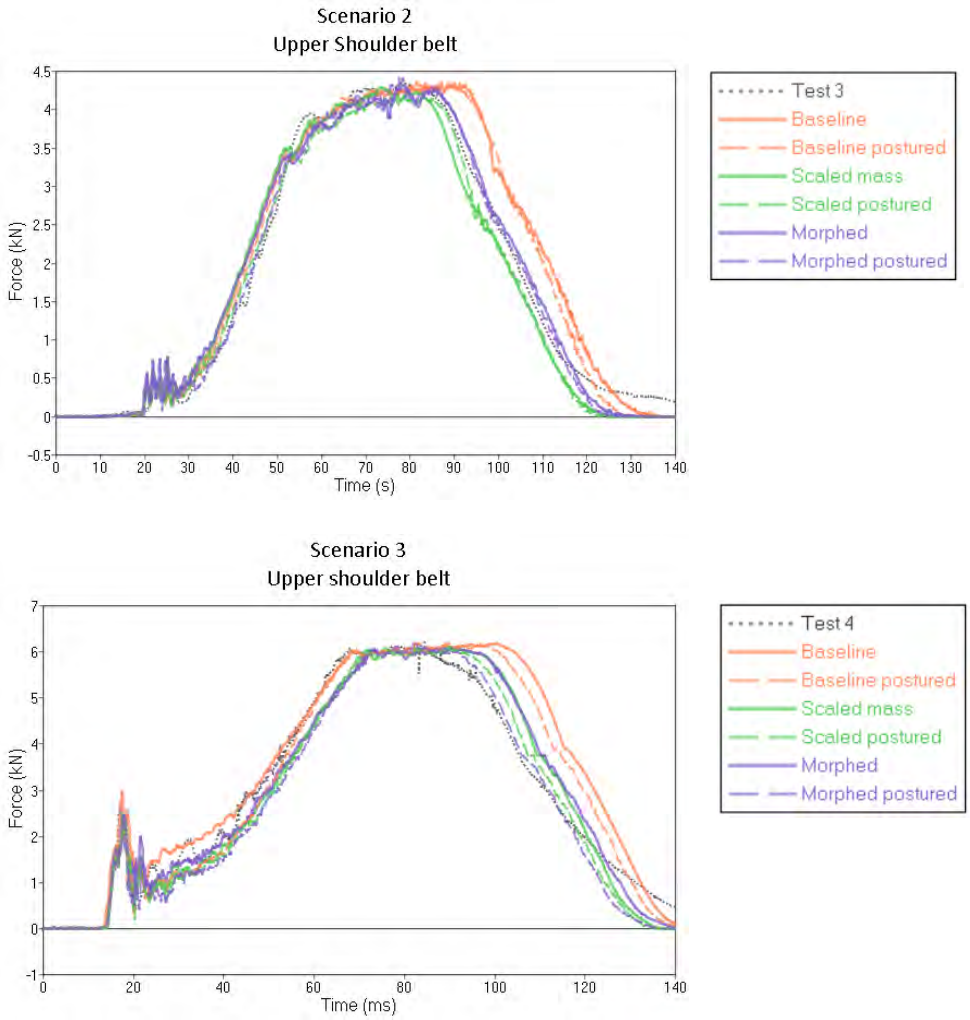

Fig. 3: Upper shoulder belt forces (kN) for the three scenarios.

Nearside Oblique Impacts

In these load cases, the PMHSs A, B and C were exposed to a nearside oblique impact at 30°. Due to the impact conditions, a significant lateral displacement was obtained.

A good biofidelity (CORA score >0.8 according to the rating stipulated in ISO/TR 18571) was observed for the head displacement of the most personalised versions (0.733 and 0.847 for the morphed postured model version in both Scenarios 1 and 2, respectively), which decreased progressively along the spine until the H-Point, in which poor CORA score (≤0.58) with the physical tests was found (0.387 and 0.495 for the morphed postured version).

The predicted displacement of T1 in Z-direction differed from the measured Z-displacement in the physical tests. In all simulations T1 moved downwards, while PMHS T1 moved slightly upwards in two of the three PMHS tests, only in one of the tests carried out in the Scenario 1, T1 follows the same tendency predicted by simulation. Consequently, a poor correlation for the T1 Z displacement was obtained, which decreased as the level of personalisation increased.

Similar patterns were obtained for the T8 behaviour. The occupants T8 tended to move upwards or keep a constant Z-coordinate during the PMHS tests. Thus, in all versions of the model, THUMS T8 moved below the Z-coordinate measured in the physical tests.

The highest CORA score for the H-Point was obtained for the morphed non-postured model in both Scenarios 1 and 2. Due to one of the retroreflective markers located on the H-Point was covered by the restrain system at 65 ms in the Scenario 2, H-Point displacement and CORA score were computed only until that time (see Fig. 2(A)).

Full frontal impact

The third load case consisted of a full frontal impact with a restraint system composed by two separated sections of seatbelt. The diagonal portion and the lap portions of the belt were separated at the buckle. In this case, the analysis was carried out in the sagittal plane only, since there was no available information about the lateral kinematics. Unlike the previous tests, the landmarks studied were left EAM, shoulder and knee, instead of Head CoG, T1, T8 and H-Point, as indicators of the head, upper spine and pelvis displacement respectively.
As with the two previous scenarios, the CORA score for the head displacement was between 0.78 (for the baseline version) and 0.941 (for the morphed postured version). The shoulder moved upwards during the PMHS test, in the same way as in the oblique impacts, whereas the THUMS model predicted downward movement. Finally, poor CORA scores were obtained for the knee displacements (0.407 in the case of the baseline model version and 0.534 for the most personalised version of the model, which is the morphed version), similar to the values obtained for the H-Point in the oblique tests.

IV. DISCUSSION

All personification techniques improved the predicted kinematics of the model, but to a different extent depending on the evaluated landmarks and the reference axis. For all scenarios, the highest CORA score was obtained for the morphed and postured model. Generally, the CORA score for the head was higher than for T1, T8, knee and pelvis. One explanation can be that the human body model in previous validation efforts was correlated and validated mainly for head displacement. The reason for that can be that there is less PMHS validation data available for T1, T8 and pelvis than for the head, therefore less validation efforts were put in to validate the prediction of T1, T8, and pelvis kinematics [1]. This fact highlights the need of continued efforts to generate more PMHS data for model validation.

The influence of personification techniques was greater in those cases in which the subject characteristics differ the most from the baseline THUMS model. For instance, this fact can be seen in the CORA score of Scenario 2 in which morphing shows a greater improvement in predicted kinematics than posturing compared to the baseline version. However, the morphed postured version (which involves all personification strategies) shows an improved rating compared to the corresponding PMHS test, as happened in all three scenarios. In the case of Scenario 1, the THUMS weight and shape most closely resembled the occupant's characteristics, but the pre-impact posture of the PMHS differed the most from the baseline model, as can be seen in Fig. 2 and Table II. Due to that, posturing has a greater influence on the kinematic response than the other strategies (mass scaling and morphing).

Nevertheless, personification of the THUMS model increased the agreement (higher CORA score) between the predicted and measured displacements more for the full frontal load cases than for the oblique load case. This despite the fact that the weight, shape and posture of the baseline THUMS model was more similar to the PMHSs in the full frontal load case. This fact can be explained looking into the CORA analysis of the three axis separately, available in Table I(A), Table II(A) and Table III(A) (see Appendix). In general, the personification techniques barely improved the lateral kinematics, which is consistent with the findings by [5]. Only in the Scenario 1, an improvement of the T8 and H-Point correlation was observed when the mass was adjusted to that of the PMHS. Regarding the X-axis, posturing and mass scaling lead to similar improvements in terms of the head kinematics, while the pelvis forward displacement was only sensitive to the mass scaling. The lowest similarity of results was observed for the pelvic vertical displacement which was little influenced when morphing. This effect can be due to the fact that one of the parameters used during the morphing of the models was the buttock circumference and the volume of flesh was significantly reduced with this strategy, hence, the pelvis displacement was more restricted because the contact between the pelvic bone and the lap belt was less cushioned by the soft tissues in the morphed versions.
In any case, poor agreement between predicted and measured pelvis displacement (lowest CORA score) was obtained. This fact can be due to several factors. One of these factors can be due to the modelling. The HBM was positioned onto the seat by means of a pre-simulation with a subsequent export of the node coordinates into the crash simulation without including the initial strains and stresses. This means that the model is not in equilibrium at t_0 and the friction to the seat might be underestimated. Another reason for the poor CORA outcome for the H-point can be due to the HBM's buttock flesh modelling. In the sled tests, the "pelvic bone" information was

approximated as the H-Point marker located bilaterally on the flesh in the same Y-coordinate of the greater trochanter. The node followed during the simulations was selected according to that in all model versions. Either the pelvic bone or the buttock flesh (or both) can be inducing this deviation. A mesh quality check was done to the morphed and baseline models in order to identify potential discrepancies. The results showed that the mesh quality was unaffected by the morphing process.
Best agreement between predicted and measured response was obtained for the most personalised model. Nevertheless, future studies could also include other personalization strategies.

The HBM materials and geometry correspond to an adult male and PMHSs at the time of death were 64±4 year-old for the oblique impact load cases and 39 year-old occupant in the full-frontal impact, thus the material properties of the default HBM can play an important role in the observed discrepancies, since only density has been changed in the scaled mass version. Further, according to the autopsy of the PMHSs done after the sled tests (available in [11-12]), rib and clavicle fractures were observed. This can result in larger deformation of the thorax, which was not represented in the simulations. That can be one of the reasons why the X-displacement (see displacement time history provided in the Appendix) of T1, T8 and shoulder is underpredicted in the more personalised model versions.

Another age related aspect that could be considered in future studies is age related changes in body composition. The Anthropometric Survey of U.S. Army Personnel (ANSUR) anthropometric database used to predict some of the missing anthropometric measurements, is based on younger subjects which are probably more fit than the occupants of these experiments, thus, the muscles/fat/bone volume proportions might differ resulting in a non-accurate morphing of the skeleton. The bones geometry extracted from a seating position CT scan would reveal possible geometrical differences between the HBM and PMHSs.

V. CONCLUSIONS

For the load cases included in this study, the more personalised the human body model was, greater the agreement between the predicted and measured kinematics. The personification have a grater influence when the HBM characteristics differ the most from the occupants.
Few improvements (only T8 and H-Point in the mass scaled model versions) were related to the lateral displacement of the observed anthropometric landmarks, thus the lateral kinematics were not sensitive to the studied personification strategies.
The lower spine kinematics is not being correctly predicted by the HBM and more effort should be done on the model validation.
This study demonstrates that the combination of the personification techniques improves the accuracy of the prediction of the occupant's kinematic and has the potential to cover a higher percentage of the population, which is not represented by the baseline models.

VI. ACKNOWLEDGEMENT

The authors thank the donors and their families for their generous act, which was essential for this study. The authors acknowledge Autoliv Research and SAFER (Vehicle and Traffic Safety Centre at Chalmers University) in Sweden for the technical resources and funding which was fundamental for the development of this study. The authors extend their thanks to Ludwig-Maximilians Universität (LMU) in Germany for their technical assistance. This study was partially funded by the Instituto Aragonés de Fomento (IAF) of Gobierno de Aragón in Spain.

VII. REFERENCES

[1] Iwamoto M, Nakahira Y, Tamura A, Kimpara H, Watanabe I, Miki K. Development of Advanced Human Models in THUMS. *6th European LS-DYNA Users' Conference*, 2007, Gothenburg, Sweden.

[2] Gayzik S, Moreno D, Vavalle N, Rhyne A, Stitzel J. Development of the Global Human Body Models Consortium mid-sized male full body model. *Injury Biomechanics Research*, pp. 39-12.

[3] Elemance. “Virtual Human Body Models,” Internet: [http://www.elemance.com/virtual-human-body-models/].

[4] Beilas P, Berthet F. An investigation of human body model morphing for the assessment of abdomen responses to impact against a population of test subjects. *Traffic Injury Prevention*, 2017, pp. S142-S147.

[5] Poulard D, Subit D, Donlon J, Lessley D, Kim T, Park G, Kent R. The Contribution of Pre-impact Spine Posture on Human Body Model Response in Whole-body Side Impact. *Stapp Car Crash Journal*, 2014, vol. 58, pp. 385-422.

[6] Poulard D, Subit D, Nie B, Donlon J, Kent R. The Contribution of Pre-Impact Posture on Restrained Occupant Finite Element Model Response in Frontal Impact. *Traffic Injury Prevention*, 2015, pp. S87-S95.

[7] Hwang E, Hu J, Chen C, Klein K, Miller C, Reed M, Rupp J, Hallman J. Development, Evaluation, and Sensitivity Analysis of Parametric Finite Element Whole-Body Human Models in Side Impacts. *Stapp Car Crash Journal*, 2016, vol. 60, pp. 473-508.

[8] PIPER EU project, “piper-project.org” [http://www.piper-project.org/], 2017/11/10 [2018/01/11].

[9] Gehre C, Gades H, Wernicke P. Objective rating of signals using test and simulation responses. *21st International Technical Conference on the Enhanced Safety of Vehicles Conference (ESV)*, 2009, Stuttgart, Germany.

[10] Iwamoto M, Kisanuki Y, Watanabe I, Furusu K, Miki K. Development of a Finite Element Model of the Total Human Model for Safety (THUMS) and Application to Injury Reconstruction. *Proceedings of IRCOBI Conference*, 2002, Munich, Germany.

[11] Iraeus J, Davidsson J, Brolin K. Recent HBM activities at Chalmers University. *Presentation at Conference: Human Body Modelling in Automotive Safety*, 2017, Berlin, Germany.

[12] Afewerki H. Biofidelity Evaluation of Thoracolumbar Spine Model in THUMS. *Chalmers University of Technology,* Gothenburg, Sweden, 2016

[13] Pipkorn B, López-Valdés F, Juste-Lorente Ó, Insausti R, Lundgren C, Sunnevång C. Assessment of an innovative seat belt with independent control of the shoulder and lap portions using THOR tests, the THUMS model and PMHS tests. *Traffic Injury Prevention*, pp. 124-130, 2016.

[14] López-Valdés F, Juste-Lorente Ó, Maza-Frechín M, Pipkorn B, Sunnevång C, Lorente A, Aso-Vizan A, Davidsson J. Analysis of occupant kinematics and dynamics in nearside oblique impacts. *Traffic Injury Prevention*, 2016, pp. 86-92.

[15] Shaw G, Parent D, Purtsezov S. Impact Response of Restrained PMHS in Frontal Sled Tests: Skeletal Deformation Patterns Under Seat Belt Loading. *Stapp Car Crash*, 2009, vol. 53, pp. 1-48.

[16] López-Valdés F, Lau J, Lamp J. Analysis of Spinal Motion and Loads During Frontal Impacts, Comparison between PMHS and ATD. *Annual Proceedings of the Association of the Advanced of Automotive Medicine (AAAM)*, 2010, p. 2010:54.

[17] Shaw G, Parent D, Purtsezov S, Lessley D, Crandall J, Kent R, Guillemot H, Ridella SA, Takhounts E, Martin P. Impact response of restrained PMHS in frontal sled tests: skeletal deformation patterns under seat belt loading. *SAE Technical Paper,* 2009 Nov 2.

[18] Wu G, Siegler S, Allard P, Kirtley C, Leardini A, Rosenbaum D, Whittle M, D'Lima D, Cristofolini L, Witte H, Schmid O. ISB recommendation on definitions of joint coordinate system of various joints for the reporting of human joint motion -- part I: ankle, hip and spine. *Journal of Biomechanics*, 2002, Vols. 35(4):543-8.

VIII. APPENDIX

Kinematic Response of the Crash Scenario 1

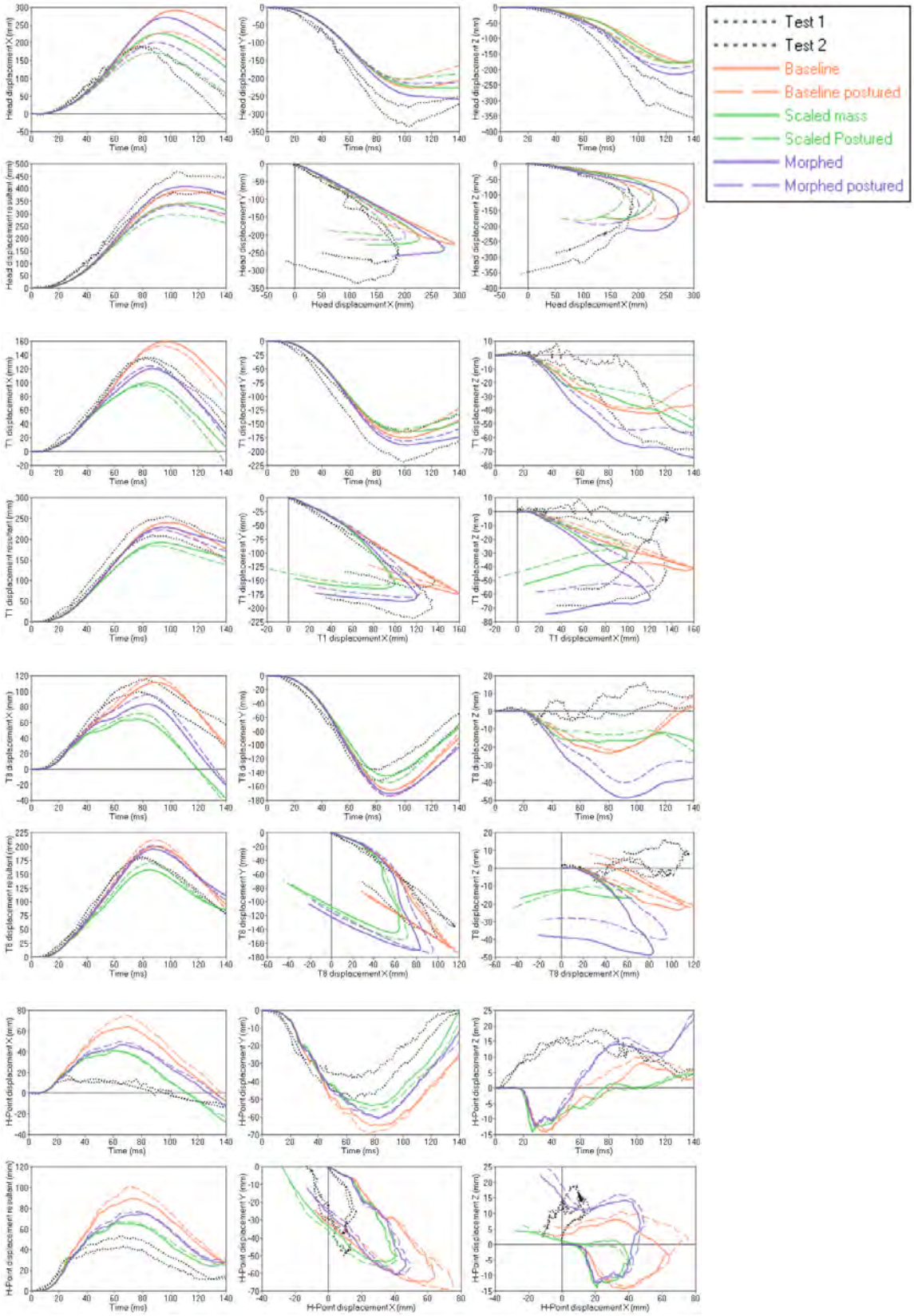

Fig. 1(A): Kinematic response of the head CoG, T1 T8 and H-Point for all simulations of the crash Scenario 1. Upper row: Displacement time history plots (X positive-forward displacement, Y positive- left displacement, Z positive-upward displacement). Lower row: Left: Resultant displacement vs. time; Centre: displacement in transverse plane; Right: displacement in sagittal plane.

Kinematic Response of the Crash Scenario 2

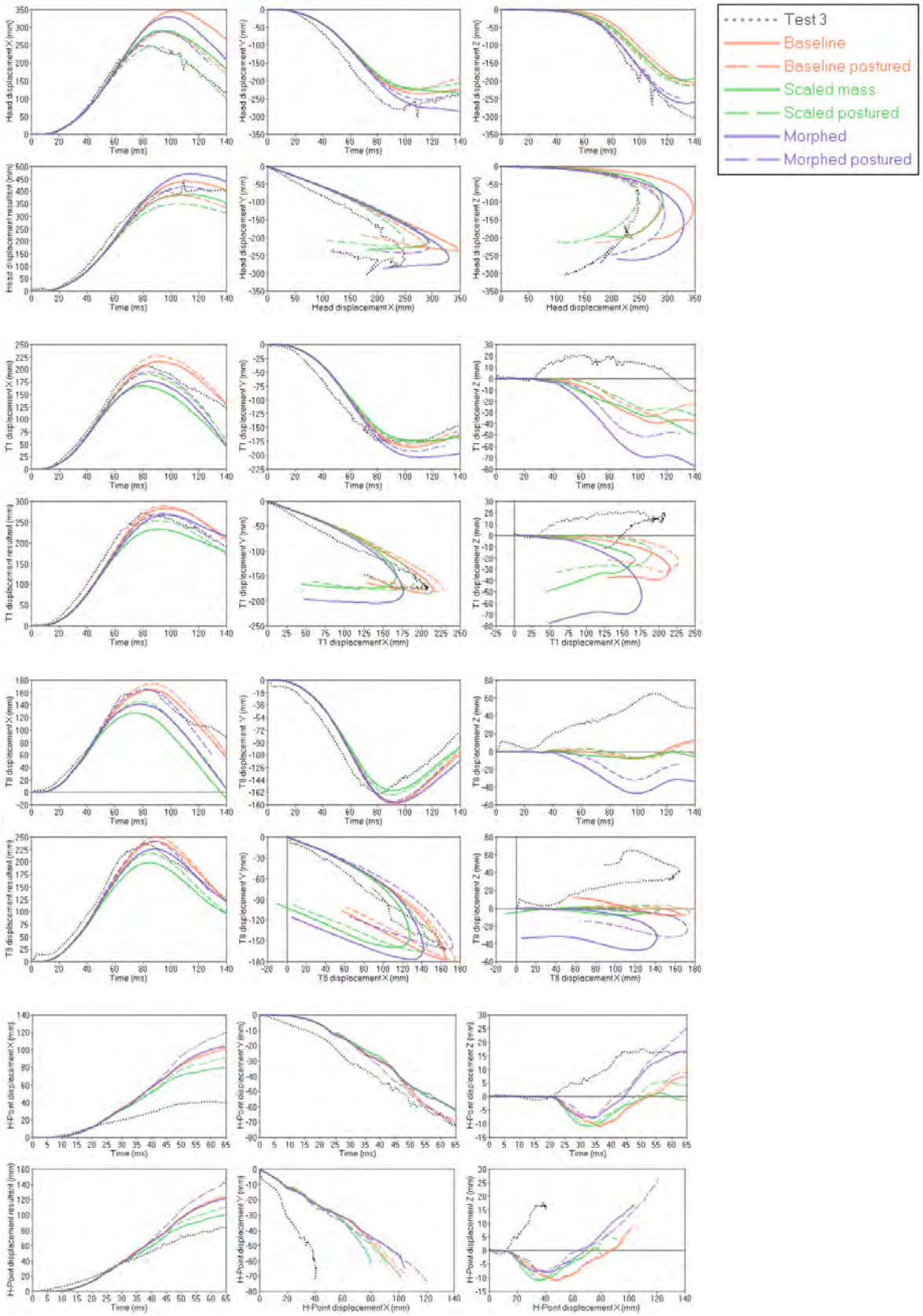

Fig. 2(A): Kinematic response of the head CoG, T1 T8 and H-Point for all simulations of the crash Scenario 2 up to 65 ms (VICON markers lost at that time). Upper row: Displacement time history plots (X positive-forward displacement, Y positive- left displacement, Z positive- upward displacement). Lower row: Left: Resultant displacement vs. time; Centre: displacement in transverse plane; Right: displacement in sagittal plane.

Kinematic Response of the Crash Scenario 3

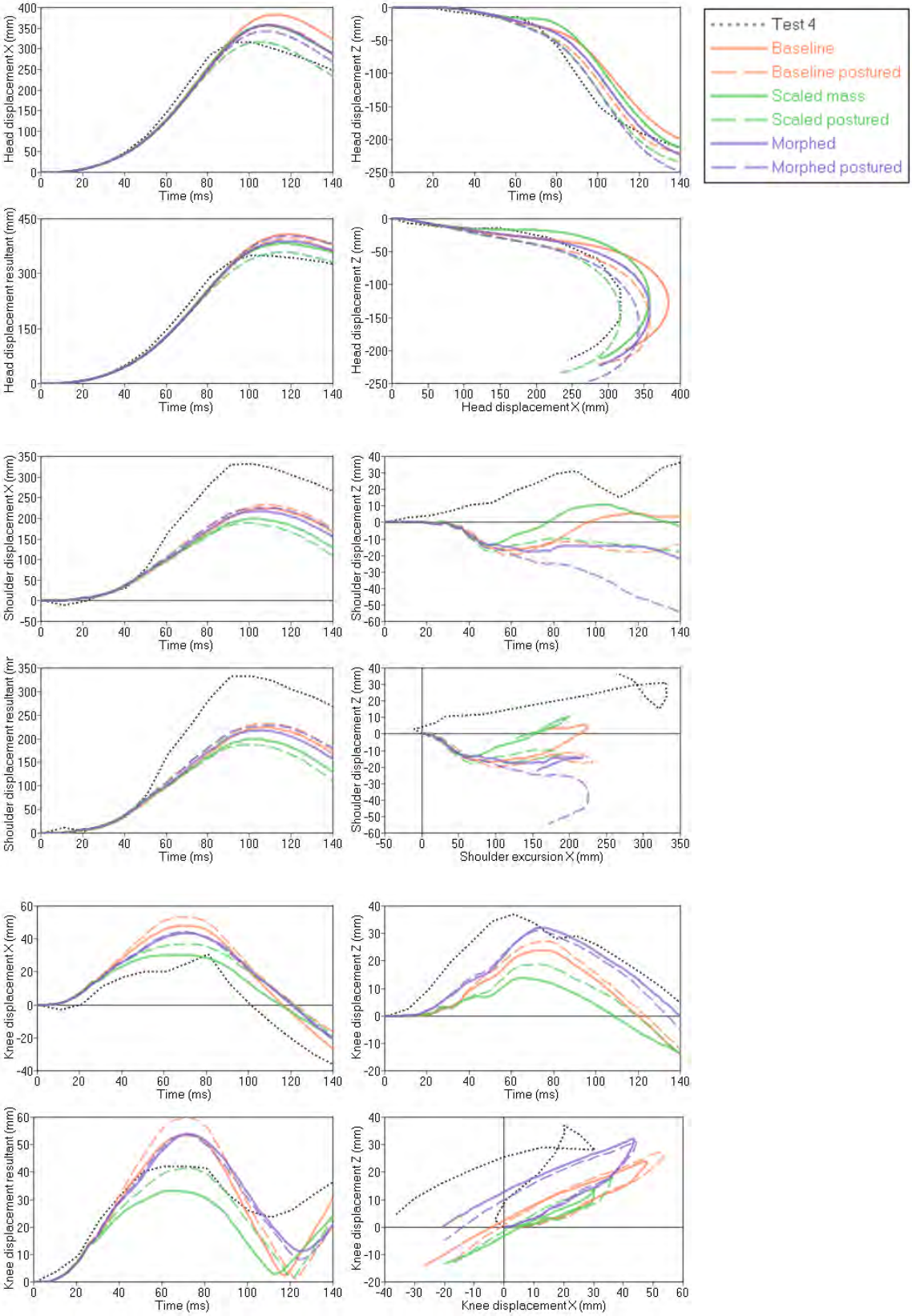

Fig. 3(A): Kinematic response of the EAM, Shoulder and Knee for all simulations of the crash Scenario 3. Upper row: Displacement time history plots (X positive-forward displacement, Z positive- upward displacement). Lower row: Left: Resultant displacement vs. time; Right: displacement in sagittal plane.

CORA Score

TABLE I(A)

CORA SCORE FOR THE SELECTED LANDMARKS IN SCENARIO 1.

THE HIGHEST VALUES OBTAINED FOR THE SELECTED LANDMARKS HAVE BEEN HIGHLIGHTED.

MODEL VERSION		BASELINE	SCALED MASS	MORPHED	BASELINE POSTURED	SCALED MASS POSTURED	MORPHED POSTURED
Total rating		0.644	0.648	0.650	0.664	0.675	0.684
Head		0.665	0.702	0.704	0.687	0.763	0.733
	Head_X	0.535	0.618	0.552	0.594	0.815	0.712
	Head_Y	0.775	0.771	0.783	0.789	0.785	0.765
	Head_Z	0.685	0.717	0.776	0.676	0.689	0.721
T1		0.7	0.699	0.687	0.735	0.685	0.735
	T1_X	0.712	0.696	0.89	0.772	0.625	0.925
	T1_Y	0.79	0.777	0.796	0.806	0.794	0.798
	T1_z	0.597	0.623	0.377	0.627	0.635	0.482
T8		0.605	0.524	0.542	0.602	0.529	0.581
	T8_X	0.844	0.458	0.685	0.844	0.498	0.818
	T8_Y	0.76	0.895	0.732	0.75	0.867	0.723
	T8_Z	0.212	0.218	0.208	0.21	0.223	0.204
H-Point		0.332	0.388	0.4	0.341	0.376	0.387
	H-Point_X	0.246	0.377	0.278	0.228	0.374	0.266
	H-Point_Y	0.518	0.622	0.562	0.506	0.589	0.554
	H-Point_Z	0.231	0.165	0.36	0.288	0.164	0.342

TABLE II(A)

CORA SCORE FOR THE SELECTED LANDMARKS IN SCENARIO 2.

THE HIGHEST VALUES OBTAINED FOR THE SELECTED LANDMARKS HAVE BEEN HIGHLIGHTED.

MODEL VERSION		BASELINE	SCALED MASS	MORPHED	BASELINE POSTURED	SCALED MASS POSTURED	MORPHED POSTURED
Total rating		0.638	0.653	0.688	0.673	0.704	0.715
Head		0.698	0.768	0.829	0.794	0.840	0.847
	Head_X	0.740	0.841	0.762	0.854	0.983	0.859
	Head_Y	0.732	0.711	0.775	0.733	0.723	0.755
	Head_Z	0.622	0.751	0.950	0.794	0.814	0.926
T1		0.612	0.572	0.593	0.608	0.639	0.628
	T1_X	0.897	0.806	0.867	0.866	0.955	0.975
	T1_Y	0.726	0.696	0.732	0.717	0.705	0.730
	T1_z	0.212	0.214	0.181	0.241	0.256	0.178
T8		0.638	0.624	0.622	0.623	0.637	0.663
	T8_X	0.953	0.742	0.873	0.906	0.90	0.994
	T8_Y	0.835	0.881	0.825	0.834	0.883	0.852
	T8_Z	0.127	0.250	0.168	0.130	0.129	0.142
H-Point		0.421	0.425	0.480	0.420	0.428	0.495
	H-Point_X	0.210	0.225	0.20	0.201	0.199	0.196
	H-Point_Y	0.649	0.625	0.645	0.644	0.638	0.639
	H-Point_Z	0.405	0.395	0.595	0.413	0.423	0.66

TABLE III(A)
CORA SCORE FOR THE SELECTED LANDMARKS IN SCENARIO 3.
THE HIGHEST VALUES OBTAINED FOR THE SELECTED LANDMARKS HAVE BEEN HIGHLIGHTED.

MODEL VERSION		BASELINE	SCALED MASS	MORPHED	BASELINE POSTURED	SCALED MASS POSTURED	MORPHED POSTURED
Total rating		0.565	0.637	0.684	0.654	0.679	0.713
Head		0.78	0.834	0.889	0.832	0.931	0.941
	Head_X	0.941	0.961	0.948	0.947	0.929	0.948
	Head_Z	0.62	0.707	0.83	0.716	0.933	0.934
Shoulder		0.359	0.459	0.484	0.498	0.451	0.494
	Shoulder_X	0.654	0.673	0.712	0.729	0.655	0.721
	Shoulder_Z	0.064	0.245	0.256	0.267	0.247	0.268
Knee		0.407	0.399	0.552	0.416	0.388	0.534
	Knee_X	0.392	0.569	0.389	0.345	0.416	0.386
	Knee_Z	0.422	0.228	0.715	0.488	0.359	0.682

TABLE IV(A)
PEAK EXCURSIONS (mm) FOR THE SELECTED LANDMARKS IN SCENARIO 1.

	TEST 1	TEST 2	BASELINE	SCALED MASS	MORPHED	BASELINE POSTURED	SCALED MASS POSTURED	MORPHED POSTURED
Head	390	468	394	342	409	339	295	333
T1	209	254	240	192	228	229	184	222
T8	178	181	200	157	195	212	169	201
H-Point	43	53	89	65	74	101	67	77

TABLE V(A)
PEAK EXCURSIONS (mm) FOR THE SELECTED LANDMARKS IN SCENARIO 2.

	TEST 3	BASELINE	SCALED MASS	MORPHED	BASELINE POSTURED	SCALED MASS POSTURED	MORPHED POSTURED
Head	401	440	386	471	385	350	419
T1	273	283	232	267	289	253	271
T8	238	241	199	226	250	217	241
H-Point	84	130	101	125	133	112	142

TABLE VI(A)
PEAK EXCURSIONS (mm) FOR THE SELECTED LANDMARKS IN SCENARIO 3.

	TEST 4	BASELINE	SCALED MASS	MORPHED	BASELINE POSTURED	SCALED MASS POSTURED	MORPHED POSTURED
EAM	351	407	382	389	397	358	403
Shoulder	333	224	199	218	233	188	229
Knee	42	54	33	54	59	52	54

Subject Anthropometry

TABLE VII(A)

SUBJECTS ANTHROPOMETRY IN THE SUPINE POSITION. ALL DIMENSIONS WERE MEASURED AS SPECIFIED IN THE NHTSA DATA REFERENCE GUIDE, VERSION 5, VOLUME II: BIOMECHANICAL TESTS (MAY 2001) AND EXPRESSED IN (mm)

	SCENARIO 1		SCENARIO 2	SCENARIO 3
SUPINE POSITION	PMHS A	PMHS B	PMHS C	PMHS D
Stature	1750	1690	1705	1810
Vertex-to-Symphysion Length	860	860	945	870
Top of Head to Trochanterion	830	855	845	855
Shoulder (Acromial) Height	1470	1420	1530	1500
Waist Height-Umbilicus	1050	980	1065	1065
Waist Depth-Umbilicus	170	135	152	172
Waist Breadth	263	257	302	272
Shoulder Breadth (Biacromial)	331	357	354	395
Chest Breadth 4th Rib	270	290	292	275
8th Rib	294	270	308	268
Chest Depth 4th Rib	258	195	192	188
8th Rib	224	186	185	203
Hip Breadth	292	292	319	247
Buttock Depth	167	155	178	175
Shoulder to Elbow	319	305	357	309
Forearm to Hand	248	235	443	255
Tibiale Height	485	440	460	400
Ankle Height (outside)	70	75	82	89
Foot Breadth	70	68	68	67
Foot Length	247	215	237	270
Head Length	202	197	218	204
Head Breadth	140	147	135	141
Head Height	208	195	219	191
Head Circumference	553	553	616	580
Neck Circumference	334	360	347	350
Chest Circumference 4th Rib	838	856	834	850
8th Rib	827	794	847	824
Waist Circumference (Umbilicus)	702	706	816	735
Buttock Circumference	776	722	830	890
Thigh Circumference	321	355	391	490
Lower Thigh Circumference	259	322	340	370
Knee Circumference	342	340	352	362
Calf Circumference	240	244	284	340
Ankle Circumference	242	212	202	255
Scye (Armpit) Circumference	235	253	251	255
Bicep Circumference	195	218	222	250
Elbow Circumference	222	233	239	255
Forearm Circumference	150	207	197	210
Wrist Circumference	159	159	151	172

TABLE VIII(A)

SUBJECTS ANTHROPOMETRY IN THE SEATED POSITION. ALL DIMENSIONS WERE MEASURED AS SPECIFIED IN THE NHTSA DATA REFERENCE GUIDE, VERSION 5, VOLUME II: BIOMECHANICAL TESTS (MAY 2001) AND EXPRESSED IN (mm)

SEATED POSITION		SCENARIO 1 PMHS A	SCENARIO 1 PMHS B	SCENARIO 2 PMHS C	SCENARIO 3 PMHS D
Seated Height-top of head to bottom of feet		963	1038	1040	-
Seated Head to Buttock		753	802	832	-
Seated Knee Height		216	445	442	-
Seated Hip to Knee length		392	364	387	-
Seated Chest Breadth	*4th Rib*	256	277	284	-
	8th Rib	260	270	289	-
Seated Chest Depth	*4th Rib*	240	202	201	-
	8th Rib	250	202	202	-
Seated Chest Circumference	*4th Rib*	858	865	856	-
	8th Rib	870	815	837	-
Interscye		297	293	299	-
Seated surface to T1		524	876	672	-
Top of Head to T1		201	202	273	-
Weight (kg)		47	53	57	62